Preform design for forging and extrusion processes based on geometrical resemblance

C Yang and **G Ngaile***
Department of Mechanical and Aerospace Engineering, North Carolina State University, Raleigh, North Carolina, USA

The manuscript was received on 30 August 2009 and was accepted after revision for publication on 9 December 2009.

DOI: 10.1243/09544054JEM1799

Abstract: Preform design in multi-stage forging processes is critical to ensure the production of defect-free parts. Moreover, owing to the geometry and material-flow complexities in forging processes, finding the optimal preform shapes could be difficult and time consuming. This paper proposes an efficient preform design methodology based on geometrical resemblance, which requires several finite element analysis simulation iterations to obtain a good preform shape. The initial and subsequent simulations are carried out by constructing a slightly larger part that geometrically resembles the desired part. Initial finite element analysis simulation of the larger part is performed with a reasonably guessed preform shape, whose forming defects or flash formation would be corrected in subsequent steps. Then a series of intermediate parts of similar shape and between the largest part and the desired part in size are constructed. The undeformed shape corresponding to an intermediate part can be obtained by backwards tracing of material flow from the simulation results of the larger part. This undeformed shape is then taken as the preform shape of the intermediate part. The procedure is repeated until the intermediate part is geometrically close to the desired part, which leads to the preform shape. In order to verify this preform-design methodology, several case studies on forging and extrusion processes have been carried out. The methodology has been shown to be computationally efficient, requiring as few as three finite element iterations to obtain a good preform shape.

Keywords: preform design, forging, finite element simulation

1 INTRODUCTION

In forging processes, the initial billet is deformed into the desired shape by compressive forces. Various forging parts usually have complex geometrical shapes that need intermediate passes to forge a sound part. Thus, design of preform dies and billet for the intermediate passes is critical in multi-stage forging to control forging quality, save material, eliminate subsequent processes, and reduce manufacturing cost.

In the forging industry, design of process sequences for specific parts has heavily relied on tryout, accumulated experience, and skill of the process designers. To reduce the time and cost associated with the development of forging sequences, numerous rule- and knowledge-based expert systems have been developed [**1**–**14**]. Most expert systems developed for determining forging sequences for cold- and hot-forged parts make use of rules and/or known progression sequences that can be retrieved from a database. For example, Kim and Im [**5**] developed an expert system that can produce the basic process design depending on the initial billet size, the material, or the order of upsetting and forwards extrusion. This system was also capable of process redesign based on either reduction of number of sequences by combining two stages into one, or reduction of deviations of the distribution and the level of the required forging load by controlling the forming ratios. Bakhshi-Jooybari *et al.* [**14**] proposed an intelligent knowledge-based system for designing of a dies and forging process, whereby the system compares new forging parts with those it had encountered previously. The comparison was based

**Corresponding author: Mechanical and Aerospace Engineering, North Carolina State University, Campus Box 7910, Raleigh, NC 27695, USA.*
email: gracious_ngaile@ncsu.edu; gngaile@eos.ncsu.edu

on weighting effects of process and on geometrical parameters that significantly influence the success of the forging.

Owing to a multitude of variables involved in a forging operation, there may exist different forging sequences to produce a sound part. This may involve changing parameters such as the initial diameter of the billet or the intermediate forging progression steps, e.g. upsetting, forwards extrusion, or backwards extrusion. Kim and Im [**11**] proposed a search method to determine an optimal process sequence using the controlled variables of global effective strain and required forging load at each stage. In this expert system, the search was carried out after a tree of possible process sequences was established.

Because the expert systems are rule-based and use plasticity theories, empirical formulae, approximate load calculations, etc. an optimal forging sequence that will lead to a sound part may be hard to obtain, particularly if the forged part is complicated. For this situation, expert systems have widely been used to provide initial progression sequences of forging, which are later modified/refined to ensure good material flow, complete die fill, and that other part defects associated with material flow are eliminated. Several researchers have incorporated finite element analysis (FEA) in expert systems as a verification tool for the established forging sequences [**3**, **4**].

Much effort has been directed towards direct use of FEA in determining forging sequences, particularly for parts that require few progression sequences. Park *et al*. proposed a backwards tracing method in preform design of shell nosing [**15**]. In 1989, Kobayashi *et al*. systematically developed the backwards tracing method for preform design in forging processes, based on rigid-viscoplastic finite element methods [**16**]. The preform shape can be computed by detaching boundary nodes from the die contact in an assumed sequence or based on some criterion. The method was successfully applied to the preform design of an axisymmetrical H-shaped forged part [**17**]. However, the validity of backwards tracing highly depends on the node-detach criteria for the deformation path. Zhao *et al*. [**18**, **19**] proposed two detach criteria based on contact history and shape complexity. The detach criteria were, however, limited to specific forging parts. Chang and Bramley [**20**] proposed a methodology for detaching contact areas from the die surface by combining the upper-bound method with the finite-element (FE) procedure. The premise of this detach criterion was that during forwards simulation, the contact areas between workpiece and dies increase along the cavities. This contacting sequence can thus be inverted in reverse simulation, i.e. nodes are detached along cavities from the deepest area. Although this method was successfully employed on a plane-strain problem, it was difficult to obtain smooth boundary shape via the FE procedures.

Researchers have attempted to optimize forging preforms using sensitivity analysis. The objective function in the sensitivity analysis is to minimize underfill, eliminate barrelling, or decrease the deviation of the state variables, whereas the design variables are coordinates of the control points of shape edges. Badrinarayanan and Zabaras developed a sensitivity analysis for large deformation of hyperelastic viscoplastic solids for optimization of extrusion die shape to achieve a more uniform distribution of the state variables on the extruded part [**21**]. Fourment and Chenot suggested a shape optimization method for the initial shape of the billet as well as the shape of preform die of a two-step forging operation [**22**]. Zhao *et al*. optimized the die preform shape to minimize the difference between actual forging shape and the desired final forging shape, based on sensitivity analysis [**23**]. Srikanth and Zabaras optimized the shape of the initial billet to minimize the barrelling in open die forging, by sensitivity analysis for the single-stage problem [**24**]. Zabaras *et al*. developed a sensitivity method to optimize the die preform shape for multi-stage metal-forming processes [**25**]. Vieilledent and Fourment proposed that folding defects could be avoided by minimizing the sum of the effective strain rates on the surface of the workpiece [**26**]. Castro *et al*. adopted the direct differentiation method to obtain sensitivity information in preform optimization design of a two-step forging process [**27**].

Preform optimization based on sensitivity analysis is an efficient algorithm to find a local optimal preform shape, but it requires gradient information of the objective function with respect to the design variables. To obtain this information, several non-gradient-based preform optimizations have been proposed. Castro *et al*. adopted a genetic algorithm to eliminate the barrelling in the hot-forging process [**28**]. Thiyagarajan and Grandhi proposed an optimization algorithm for a three-dimensional (3D) preform shape design based on the response surface method, in which the preform shape was treated as a linear combination of various billet shapes called basis shapes, where the weights for each basis shape were used as design variables [**29**]. Hong *et al*. suggested an iterative preform design method to reduce flash formation and forging load. The optimal preform shape was found by iteratively mapping the shape of the formed flash of reduced size to the initial billet shape [**30**]. Preform design methodologies that are more robust and efficient are needed. This paper proposes an efficient preform design method based on geometrical resemblance, which may take only a few iterations to find a good preform shape.

2 PREFORM DESIGN BASED ON GEOMETRICAL RESEMBLANCE METHODOLOGY

The primary criterion in preform design of a multi-stage forging process is that the forged part should be free of defects such as die underfill, folding, laps, and fracture. The preform shape of a successfully forged part should lead to good material flow patterns to avoid any forming defects. Figures 1 and 2 illustrate the geometrical resemblance methodology in preform design. Assume that part X_a shown in Fig. 1(b) is that whose preform shape needs to be found, and Fig. 1(a) shows the optimal die preform shape found. Figure 2 shows the axisymmetric upsetting of part X_b with preform shape P_b. A curve X_a is constructed inside part X_b, the undeformed shape P_a can be obtained by backwards tracing of the material flow via FEA simulation. Figures 1 and 2 imply that the deformation process of P_a to X_a in the upsetting process of X_b (Fig. 2) is close to upsetting of P_a to X_a directly (Fig. 1) if X_a is geometrically close to X_b. When X_a and X_b are not geometrically close enough, a series of intermediate resembling shapes can be constructed to trace the preform shape of X_a.

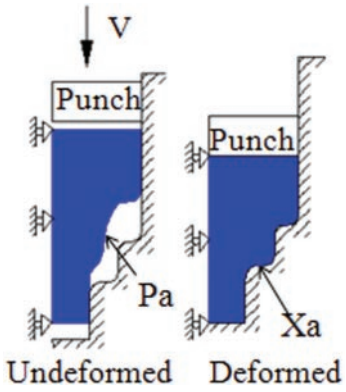

Fig. 1 Forging of part X_a

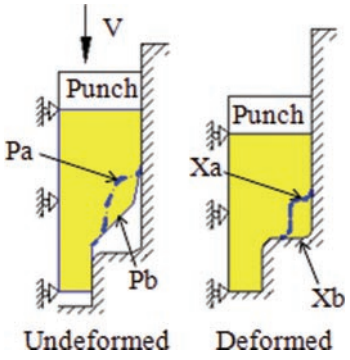

Fig. 2 Forging of part X_b

Based on the assumptions, the preform design methodology is outlined below. The illustrations for the design of preform shape P_a for part X_a are given in Figs 3 and 4.

1. Let the final shape of part X_a be known (Fig. 3): Construct a bigger part X_d that resembles X_a geometrically and contains the shape of X_a.
2. Design preform shape P_d of part X_d. In this step, the preform shape P_d does not strictly need to form part X_d without defects. Underfill and flash forming are allowed because the necessary condition is that the deformed shape X_d at least contains the shape of X_a.
3. Construct an intermediate shape X_c between X_a and X_d by the offset method $X_c = X_a + f$, where f is the offset distance. The preform shape P_c of part X_c can be obtained by tracing backwards the material flow using FEA simulation results of the process of forging X_d.
4. Construct another intermediate shape X_i (e.g., X_b) between X_c and X_a by the offset method $X_i = X_a + \alpha f$, where $\alpha < 1$. Now repeat step 3 by gradually reducing α and then finding the preform shape P_i of X_i that is close to X_a.
5. Iterate step 4 until X_i is very close to X_a. Then the preform shape P_a of X_a can be found by tracing backwards the material flow from the FEA simulation results of the forging process of P_i.

Using the proposed methodology, a reasonable preform shape can be found by a few iterations when the initial constructed part X_d is close to X_a. This method is easy to apply and can be incorporated into commercial FEA packages for preform design. This study used the commercial FE package DEFORM 2D, whose 'track point' function can track the deformation history of specific material points on the forging part. This methodology is illustrated by several case studies presented in sections 3 and 4.

3 APPLICATIONS FOR TWO-DIMENSIONAL CLOSED-DIE FORGING PROCESSES

3.1 Preform design of flashless forging of axisymmetric rib-web part

In the forging process of rib-web part, billet material is difficult to flow into rib cavity owing to the high ratio of rib height to rib thickness. Preform of the rib-web part is designed to facilitate the material flow, improve the die fill, and achieve flashless forging. Figure 5 shows an axisymmetric rib-web part with height-to-thickness ratio of 2.0. Without a preform, underfill and flash formation are observed as shown in Fig. 6(a). The billet material used to simulate this part was copper with a flow stress expressed as

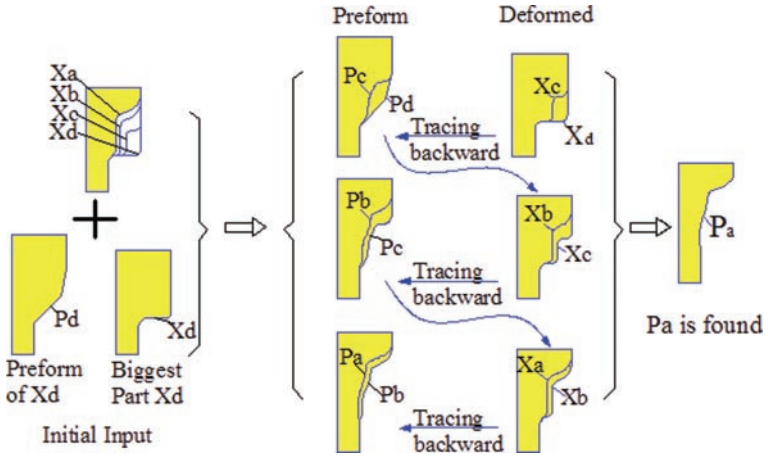

Fig. 3 Illustration of preform design of part X_a

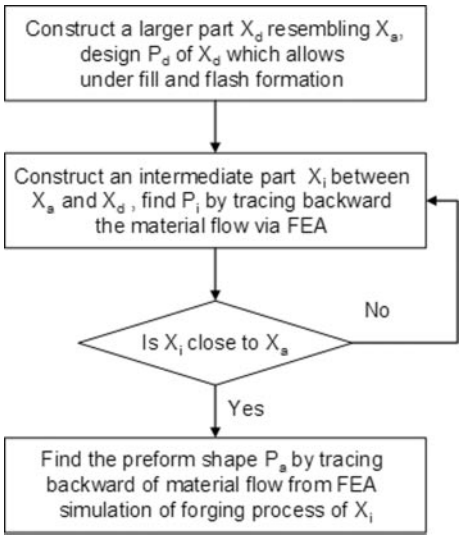

Fig. 4 Flow chart of preform design

$\bar{\sigma} = 560\bar{\varepsilon}^{0.46}$. This flow stress was obtained by compression test carried out by the authors. The proposed preform design method is applied to this part as described below.

1. For the preform design of this part, the first step is to construct a series of bigger parts X_b, X_c, X_d and design a reasonable preform shape P_d of X_d as shown in Fig. 6(c). Figure 6(b) shows a series of constructed bigger parts X_b, X_c, X_d . These parts are constructed by offsetting the top and side edges of X_a by a distance. Figure 6(c) shows the guessed preform shape P_d of part X_d. P_d has a bevel shape at the centre in order to improve the material flow. It should be noted that P_d is not strictly required to form X_d. Underfill and flash are allowed, but at least the deformed shape of P_d should contain X_c to make the backwards tracing method applicable.
2. Iteration 1. After X_d and P_d are constructed, FEA simulations are carried out to simulate the forming process of X_d. Figure 7(a) and (b) show the initial and the final steps of FE forging simulations of X_d respectively. From the results it can be seen that underfill occurs in the forming of X_d. It can be observed that the deformed shape of X_d surrounds X_c. A series of track points along X_c are made to find the preform shape P_c of X_c as shown in Fig. 7 (c) and (d).
3. Iteration 2. Use the P_c as the billet shape of X_c and simulate the forming process of part X_c (Fig. 7(e) and (f)). Then construct track points along X_b (Fig. 7(g)) to trace backwards the undeformed shape of part X_b as preform shape P_b of X_b (Fig. 7 (h)).
4. Iteration 3. Use the P_b as the billet shape of X_b and simulate the forming process of part X_b (Fig. 7(i) and (j)). Then construct track points along X_a (Fig. 7(k)) to trace backwards the undeformed shape of X_a as preform shape P_a of X_a (Fig. 7(l)).

Based on the preform shape of P_a, the initial billet shape can be found by the constant volume condition. The diameter and the height of the initial billet are assumed to be 25 mm and 16.34 mm respectively. Figure 7(m) and (n) show the initial and the final steps of the preforming simulation. Figure 7(o) and (p) show the initial and final steps of finish forging of X_a. Figure 8 shows the effective strain distribution of part X_a, where the maximum and minimum values are 3.08 and 0.268 respectively. Figure 9 shows the die loads in the both stages, where the load in preforming is about 750 kN and the load in finish forging is about 973 kN. It should be noted that a friction factor of $m = 0.12$ was assumed for all FE simulations. Experimental validation for this preform design is presented in section 5.

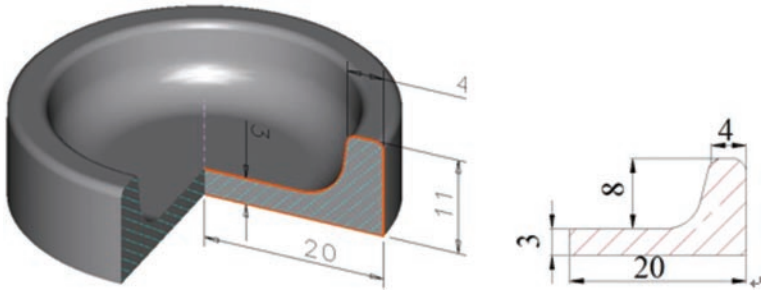

Fig. 5 Axisymmetric RIB-WEB PART with H/B = 2.0

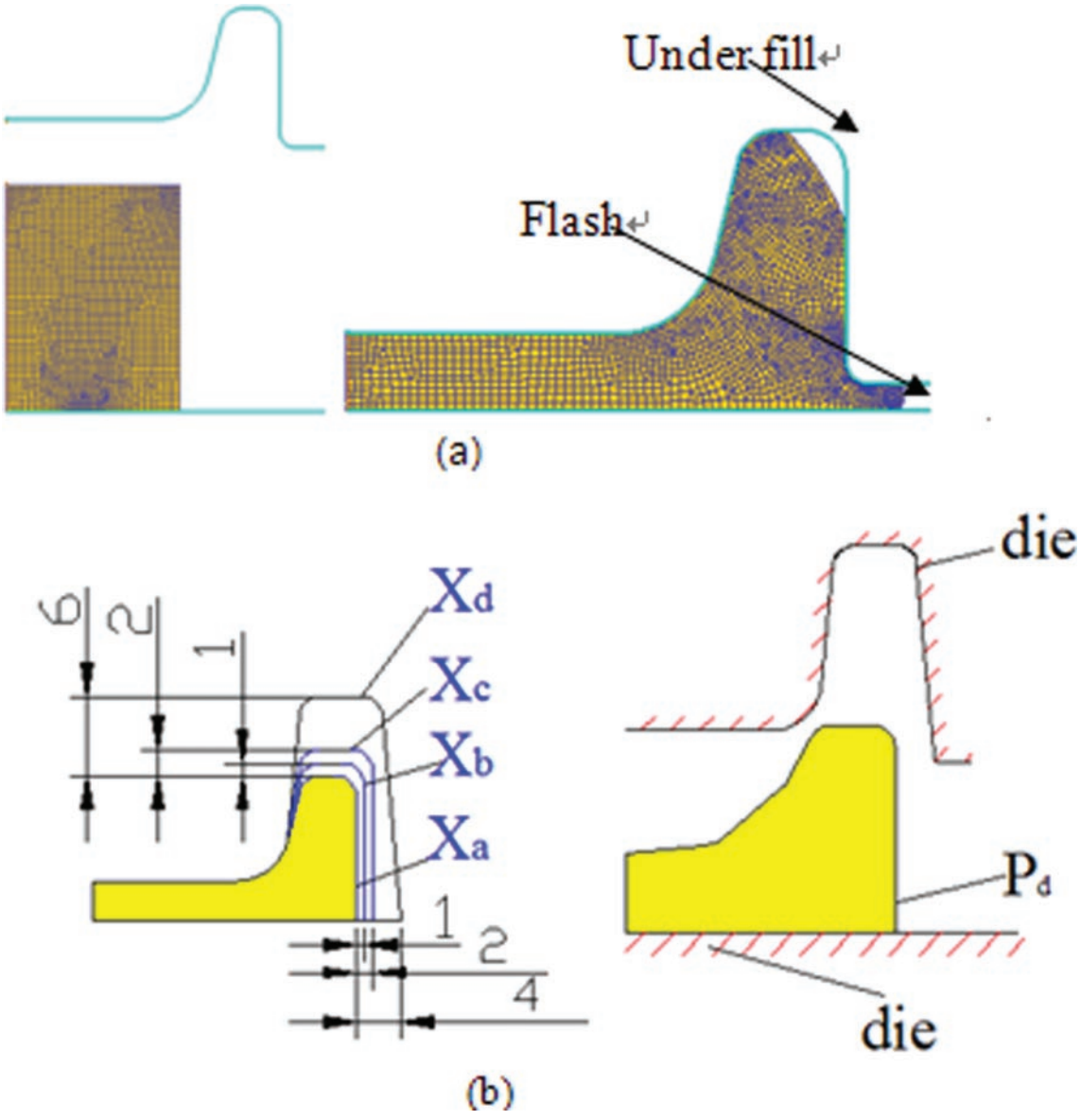

Fig. 6 (a) Defects after direct forging, (b) constructed larger parts and guessed P_d

3.2 Preform design of flashless forging of axisymmetric part with multiple ribs

Figure 10(a) shows an axisymmetric part with three ribs. The span between rib-2 and rib-3 is two times of that between rib-1 and rib-2. The rib height to width ratios are 1, 2, and 3 for the three ribs respectively. Owing to the high rib height to rib width ratio, preform stages are required to forge a flashless part. As shown in Fig. 10(c), underfill

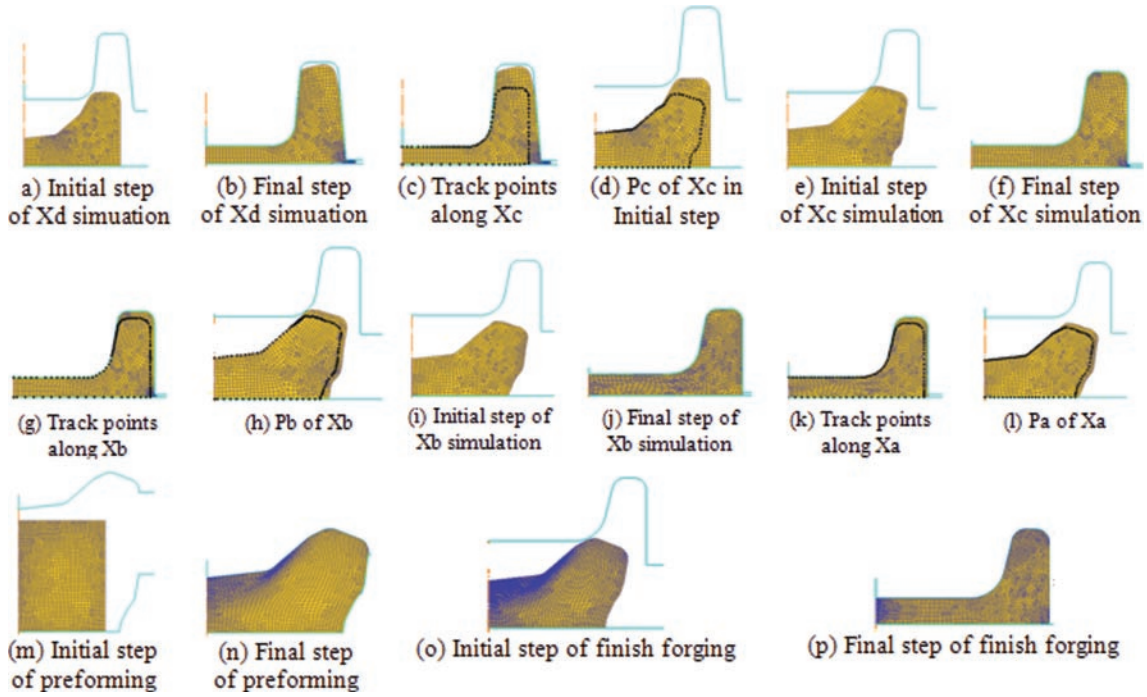

Fig. 7 Preform design of X_a by tracing backwards method

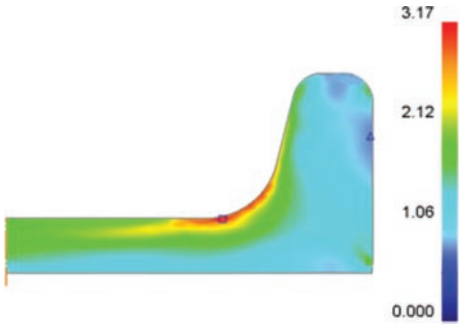

Fig. 8 Effective strain distribution of X_a

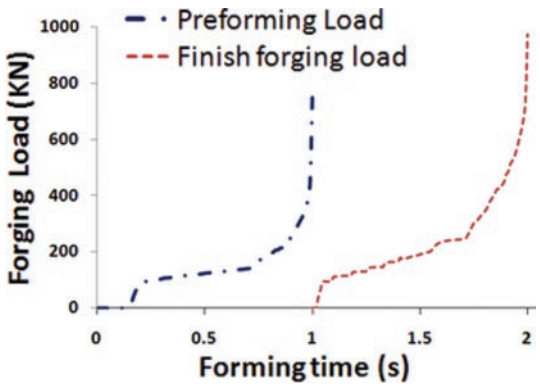

Fig. 9 Die load of preforming and finish forging

occurs and flash forms in the forging process without preform stages. The preform shape of this part can be designed with the proposed method.

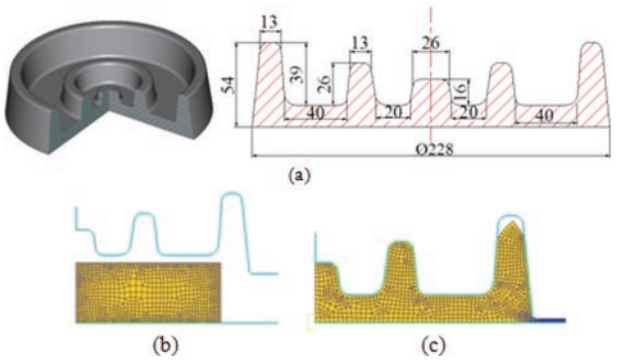

Fig. 10 (a) Axisymmetric part with multiple ribs; (b) forging process without perform; (c) defect in forging process

This part is forged at an elevated temperature to reduce the flow stress and ease the material flow in the forging process. Therefore the billet and the tool are heated to 1000 °C and 200 °C respectively. The geometrical size and the axisymmetric model of this part are shown in Fig. 10 and Fig. 11. AISI-4340 is used in the FEA simulation. The preform shape of this part can be obtained as outlined below.

1. The first step is to construct a bigger part X_c and design a reasonable preform shape P_c of X_c. Figure 10(c) shows that underfill and flash will be formed if the part is formed without a preform. This is attributable to high rib to width ratio.

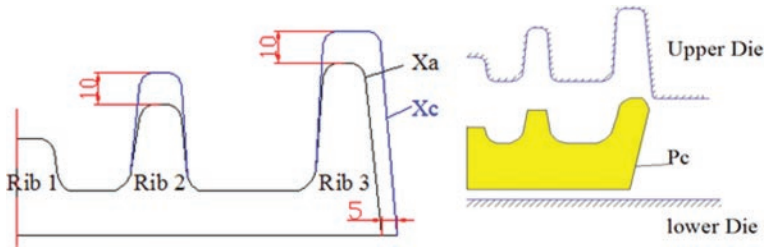

Fig. 11 Constructed X_c and guessed preform shape P_c

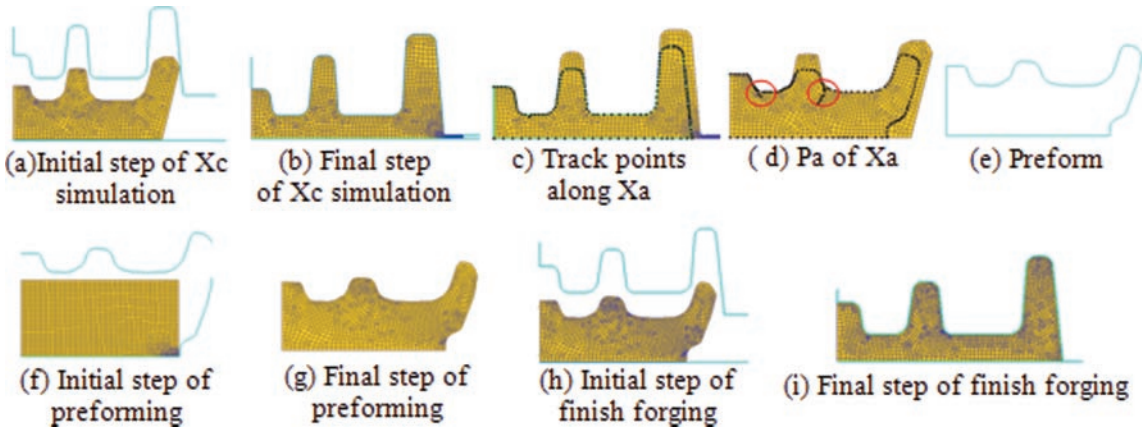

Fig. 12 Preform design of X_a by tracing backwards method

Therefore X_c is constructed by offsetting the top edge of rib-2 and rib-3 by 10 mm each and side edge of rib-3 by 5 mm (Fig. 11). The preform shape P_c of bigger part X_c is initially designed as shown in Fig. 11. However preform P_c is not strictly required to form X_c, i.e. die underfill and flash formation are allowed, but at least the deformed shape of P_c should contain X_a to make the backwards tracing method applicable.

2. After the X_c and P_c are constructed, FEA simulations are carried out to simulate the forming process of X_c. Figure 12(a) and (b) show the initial and the final steps of FEA forging simulations of X_c. It can be seen that X_c is forged completely with flash formation. Then a series of track points along X_a are made to find the preform shape P_a of X_a as shown in Fig. 12(c) and 12(d). In this problem, the intermediate shapes are not used and the preform shape is found by only one iteration due to the fact that the shapes of X_a and X_c are simple and geometrically close. Figure 12(d) shows the undeformed shape of X_a which is taken as preform shape P_a of X_a after removing some noise point marked by circles in Fig. 12(d). Figure 12(e) shows the preform shape P_a of X_a.

Once the preform shape Pa is found, the initial billet shape can be obtained by the constant volume condition. The radius and height of the initial billet is assumed to be 90 mm and 43.6 mm respectively. Figure 12(f) and (g) show the initial and final steps of the preforming simulation. Figure 12(h) and (i) show the initial and final steps of finish forging of X_a. Figure 13 shows the effective strain distribution of part X_a where the maximum and the minimum values are 3.34 and 0.276 respectively. Figure 14 shows the die loads in the preform and finish forging stages, where the loads are 2.35×10^4 kN and 2.75×10^4 kN respectively.

4 APPLICATIONS FOR TWO-DIMENSIONAL EXTRUSION AND UPSETTING PROCESSES

4.1 Preform design of cold heading of a stud

Generally the forming process of the stud requires several passes such as extrusion process, heading process, etc. In the heading process of the stud, the preform design is a critical step to avoid forming defects such as folding or underfill of the die corner. Figure 15 shows the typical forming sequences of the stud consisting of extrusion, performing, and heading process. The preformed shapes play an important role for a successful heading operation. Usually a barrel shape is used in heading process to enhance the die fill of the corner and to avoid flash formation. However, an improper barrel shape may result in folding, underfill and flash formation as shown in Fig. 16.

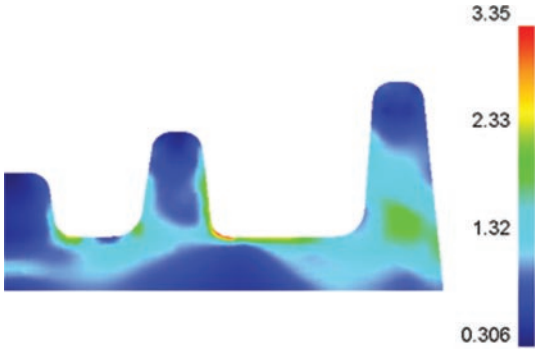

Fig. 13 Effective strain distribution

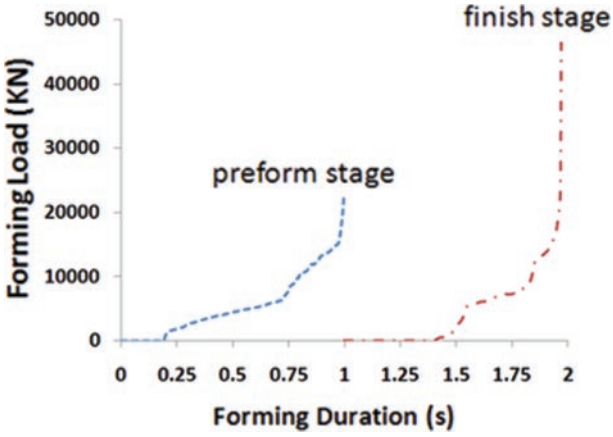

Fig. 14 Die load of perform and finish forging

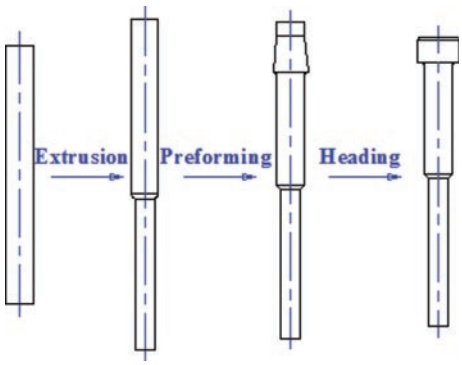

Fig. 15 General forming sequence of a stud [**31**]

1. Using the proposed method, the preform design of the stud can be carried out as described below. Material AISI 4140 is used.
2. The first step is to construct a series of bigger parts for X_c and X_b resembling the stud X_a as shown in Fig. 17 by offsetting the side edge by 2 and 4 mm respectively.
3. Then give a reasonable guess for the preform shape P_c of a bigger part X_c (Fig. 18(a)) and simulate the forming process of X_c (Figs 18(b) and 18(c)).

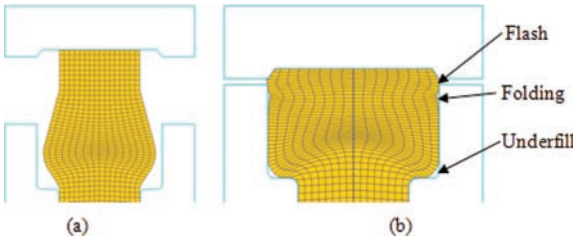

Fig. 16 (a) Preform shape, (b) forming defect of the stud in the heading pass

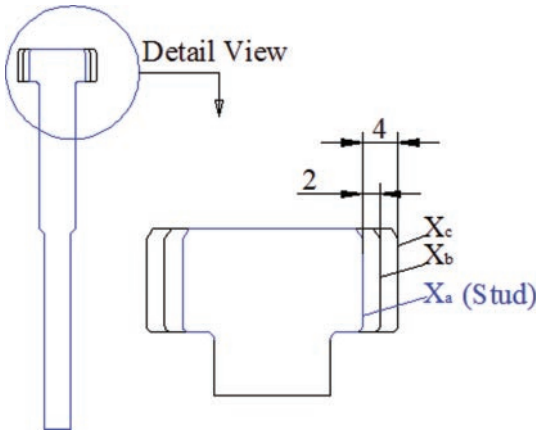

Fig. 17 Construction of a series of parts resembling the stud

4. Construct track points along X_b from the simulation results of forming of X_c (Fig. 18(d)) and trace backwards to obtain preform shape P_b of X_b (Fig. 18(e)).
5. Simulate the forming process of X_b (Fig. 18(f) and 18(g)) and construct track points along X_a (Fig. 18 (h)), then trace backwards the undeformed shape P_a of X_a which is assumed to be preform shape of X_a (Fig. 18(i) and 18(j)).
6. Simulate all three passes to verify the preform shape of X_a. (Fig. 19).

Figure 19 shows FEA simulations of three passes which verify the designed preform shapes of the stud. Figure 19 also shows the effective strain distribution for the three passes where the maximum strain is about 1.5. The forming loads for the three passes are 177 kN, 503 kN, and 1879 kN respectively as shown in Fig. 20.

4.2 Preform design of shaft upsetting process

In shaft upsetting process, improper preform shape (Fig. 21(a)) may result in folding and underfill problems near the shaft shoulder as shown in Fig. 21(b). The proposed preform design method based on the geometrical resemblance is used to find a proper preform shape for this shaft upsetting process.

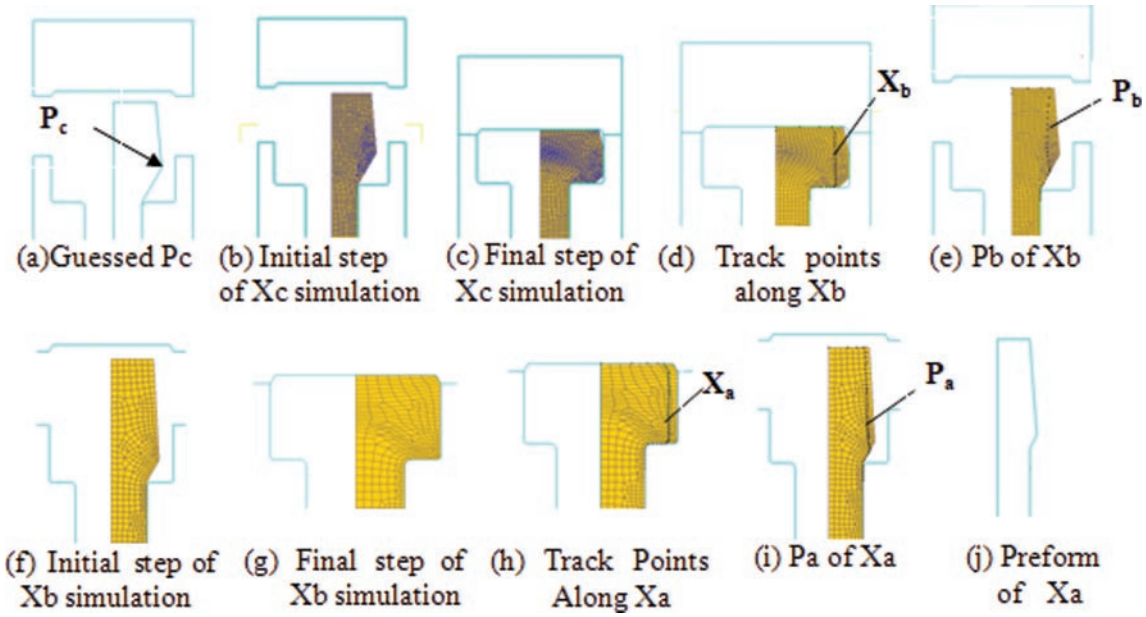

Fig. 18 Preform shape design of stud X_a

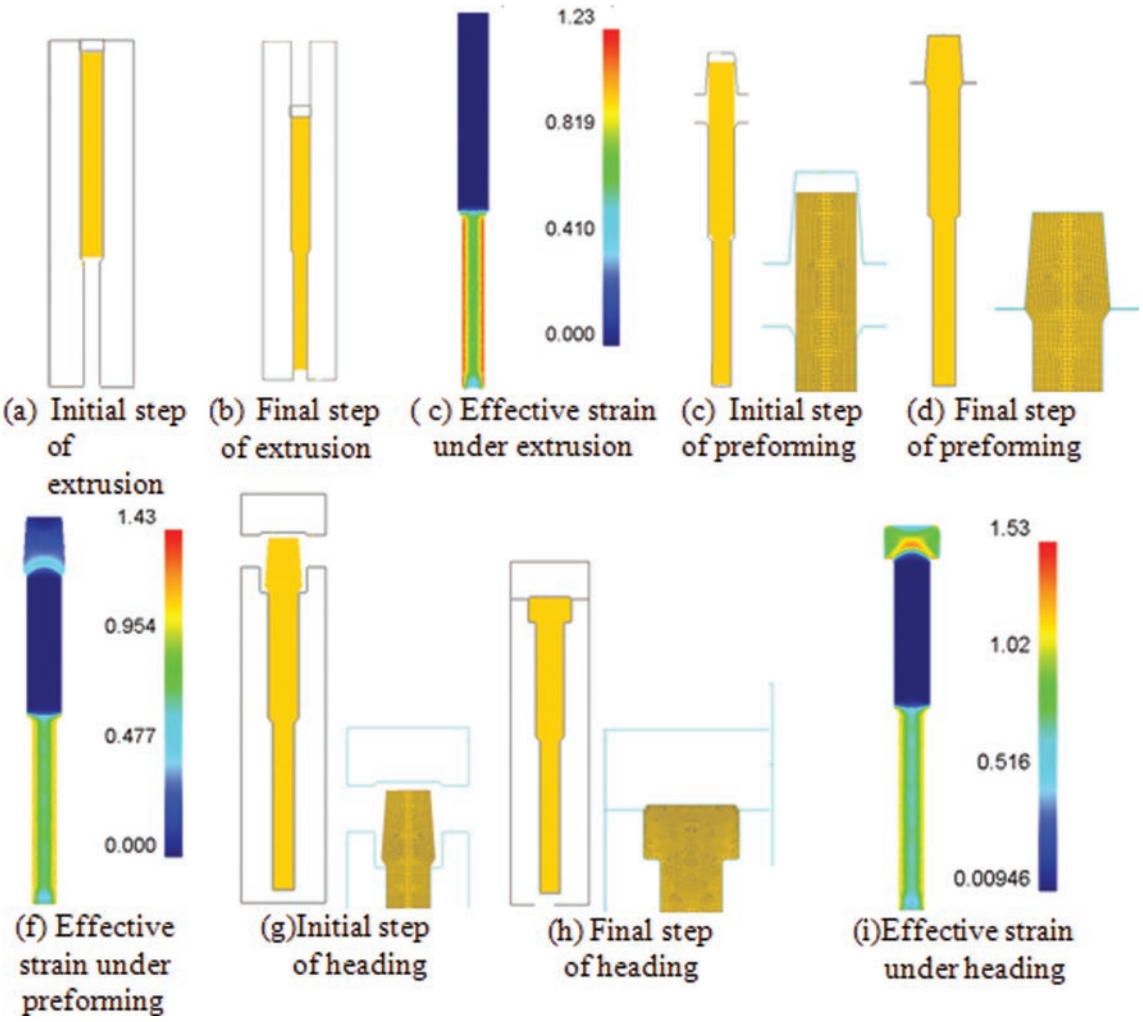

Fig. 19 FEA simulation of three passes of stud forming

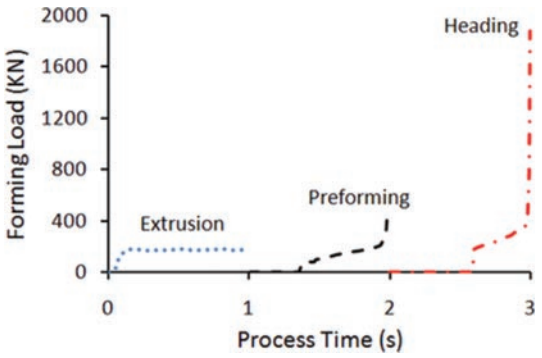

Fig. 20 Forming loads of three passes of stud forming

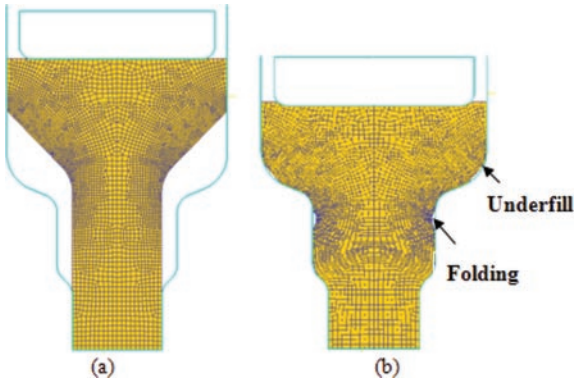

Fig. 21 (a) Improper preform shape and (b) forming defects

Owing to the axisymmetry of the shaft geometry, only half of the model (Fig. 22(a)) is used in the preform shape design. The same material AISI-4140 as in the previous application discussed in section 4.1 is used. In order to improve the formability the upsetting process is done at elevated temperature, where the billet and die are heated to 1000 °C and 200 °C respectively. Figure 22(a) shows the detailed geometrical shape and size of the shaft represented by X_a. As discussed earlier, the forming defects occur around the shaft shoulders, thus the preform shape corresponding to the shoulder feature forming is critical for the successful upsetting process. Accordingly, a series of parts having similar shoulder features with that of the shaft are constructed to find the proper preform shape P_a of shaft X_a. Using the proposed preform design method, the preform can be obtained as follows:

1. Construct a series of bigger parts X_b, X_c and X_d by offsetting the shaft shoulder feature as shown in Fig. 22(b).
2. Iteration-1. Guess a reasonable preform shape P_d (Fig. 23) for bigger part X_d (Fig. 22(b)). Then construct track points along X_c (Fig. 24(c)) to trace backwards to obtain undeformed shape of part X_c as preform shape P_c of X_c (Fig. 24(d)).

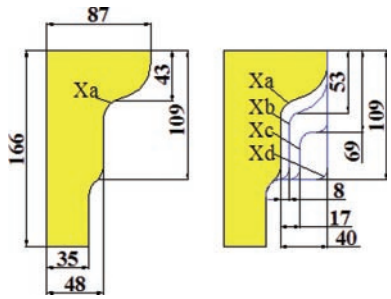

Fig. 22 (a) Half geometrical model of shaft, (b) a series of parts constructed to resemble the shaft

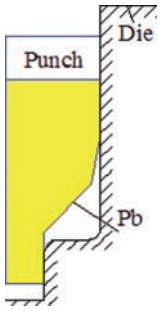

Fig. 23 Guessed preform shape P_d of shape X_d

3. Iteration-2. Use the P_c as the billet shape of X_c and simulate the forming process of part X_c (Fig. 24 (e) and Fig. 24(f)). Then construct track points along X_b (Fig. 24(g)) to trace backwards the undeformed shape of part X_b as preform shape P_b of X_b (Fig. 24 (h)).
4. Iteration-3. Use the P_b as the billet shape of X_b and simulate the forming process of part X_b (Fig. 24(i) and Fig. 24(j)). Then construct track points along X_a (Fig. 24(k)) to trace backwards the undeformed shape of X_a as preform shape P_a of X_a (Fig. 24(l)).

The basic preform shape P_a of shaft is found. However, P_a has an undesired barrelling feature (Fig. 24(l)) which gives ejection problem in the upsetting process. This bulge feature should be replaced by flat feature with the same volume. Figure 25 shows the preform shape of shaft upsetting and FEA verification results where no forming defect is found. The maximum effective strain is 3.56 as observed in Fig. 26. The effective strain and forming load for the preform and finish stages are shown in Figs 26 and 27.

Although the procedures for the FE simulations for the cases presented above were done manually, this methodology could easily be automated, i.e. after inputting the initial assumed geometries in the FE model, the next iteration stages can be carried

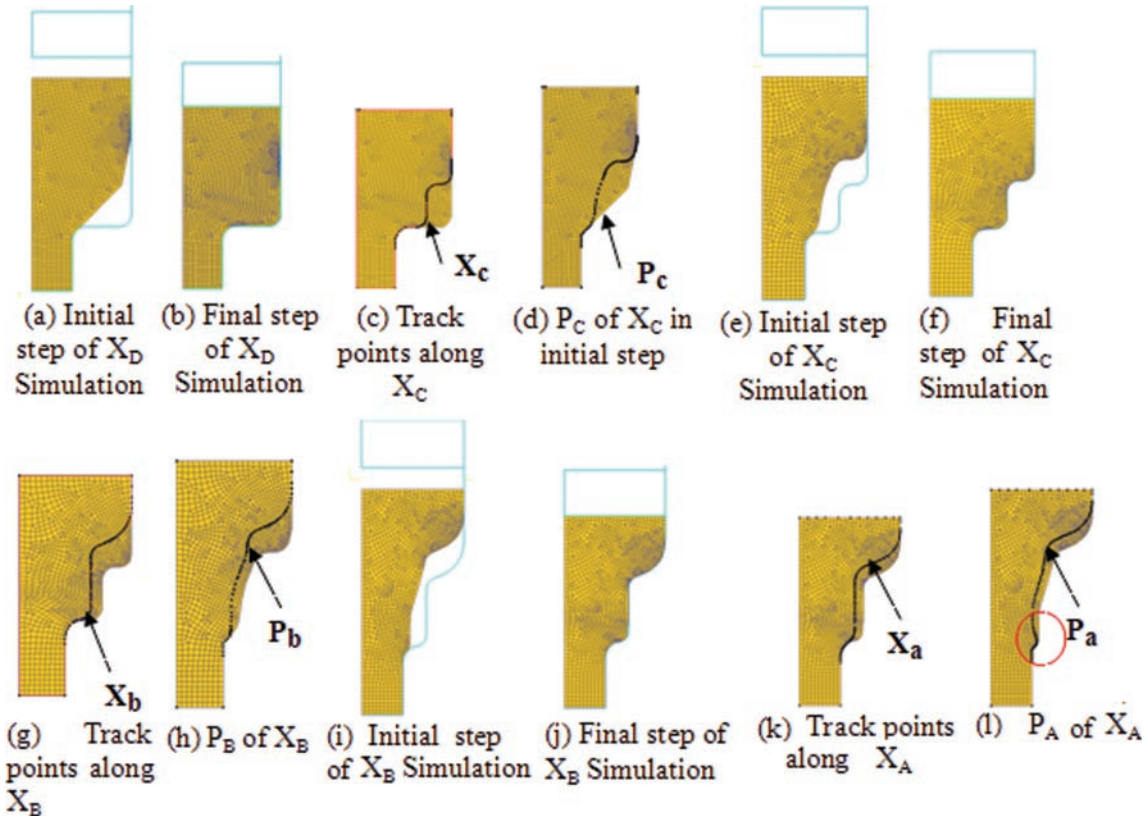

Fig. 24 Preform design of shaft upsetting process

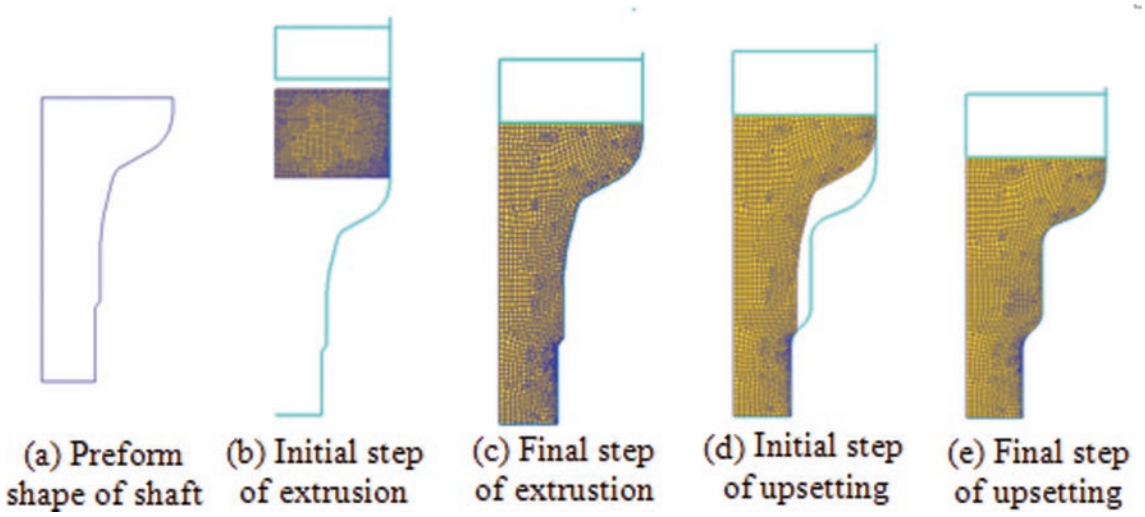

Fig. 25 FEA simualtion of two forming stages of shaft

out automatically, until an optimized preform geometry is obtained.

In sections 3.2 and 4.1, alloy steel materials AISI 4340 and AISI 4140 were used in the preform design of flashless forging of an axisymmetric part and cold heading of a stud respectively. It should be noted that these materials are usually annealed before forging is carried out to acquire the ductility needed for forging and also to ensure that the desired strength, toughness, and microstructure characteristics of the part after forging are met. Annealing of both AISI 4340 and AISI 4140 is usually carried out at temperatures between 1450 °F and 1550 °F [**32**]. These materials can also be spherodized to enhance ductility, particularly, on parts which have been work hardened, to allow them to be further worked.

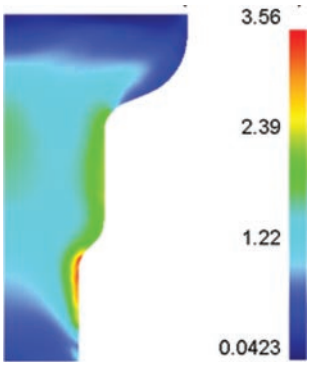

Fig. 26 Effective strain distribution of shaft

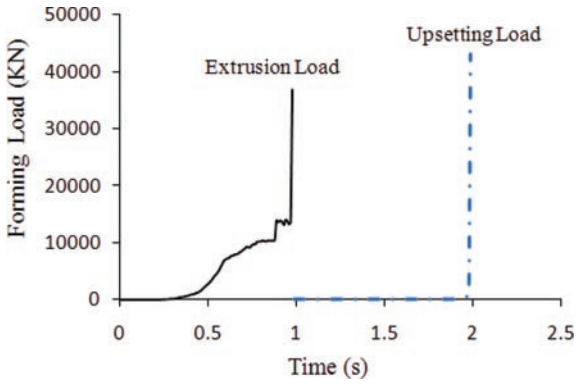

Fig. 27 Forming load of shaft upsetting process

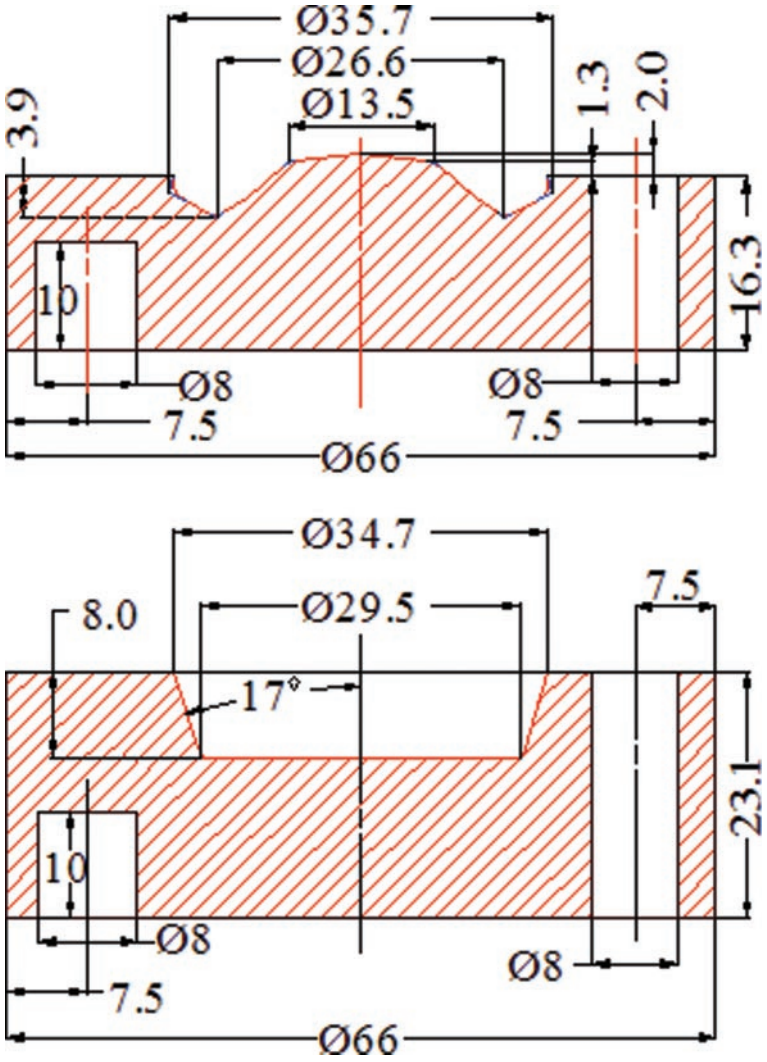

Fig. 28 Upper and lower preform dies

One of the spherodizing techniques used in industry for AISI 4140 consists of heating the steel into intercritical temperature (1360 °F–1400 °F) for 2–6 h and slowly cool below the lower critical temperature (1290 °F–1320 °F) and hold at this temperature for 8–20 h before cooling to room temperature. The cost of this heat treatment process can be significant owing to long heat treatment time [**33**].

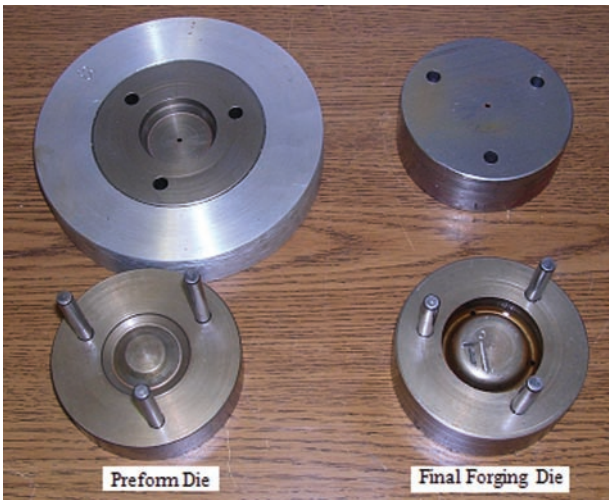

Fig. 29 Preform and final die sets

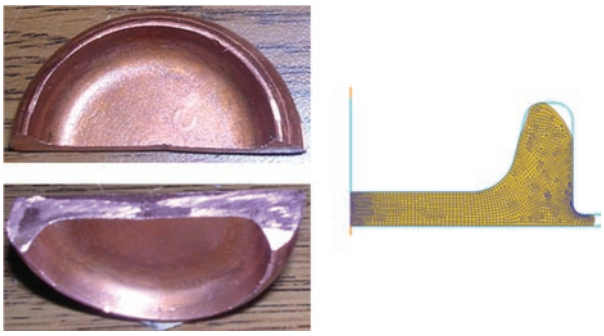

Fig. 30 Underfill and flash formation

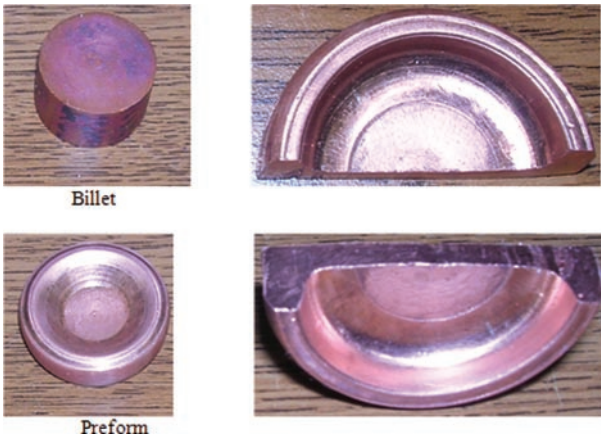

Fig. 31 Preform and final geometry

5 EXPERIMENTAL VALIDATION

Experimental validation for the preform design methodology presented earlier was carried out for flashless forming of the axisymmetric rib-web part shown in Fig. 5. A 150 ton hydraulic press was used. The preform dies were fabricated based on the preform shape obtained by FE simulations, as shown in Fig. 7. Figure 28 shows the drawings of the upper and lower preform dies, and Fig. 29 shows the actual die sets used in the experiments.

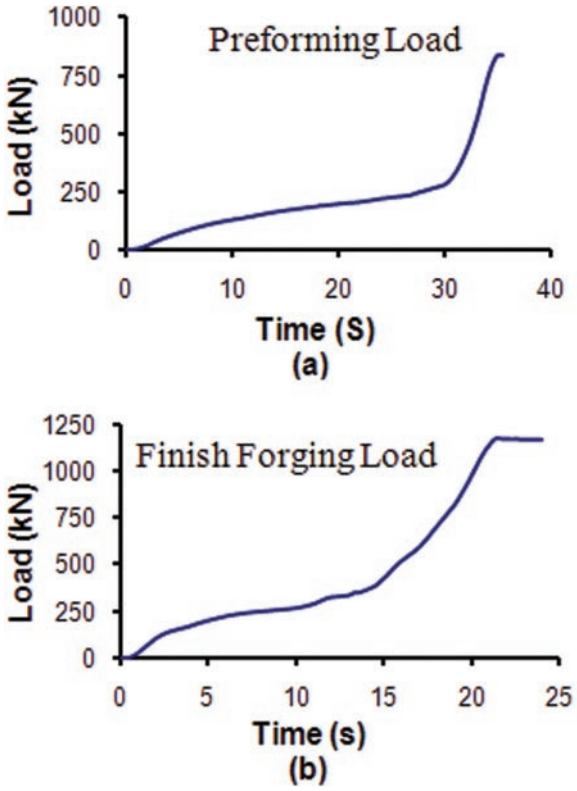

Fig. 32 (a) Preform load and (b) final forming load

5.1 Experimental procedures and test results

The material used for validation was annealed copper alloy 101. The annealing procedures were such that the samples were heated in a furnace to a maximum temperature of 1100 °F under nitrogen. The furnace was then switched off. When the temperature dropped to 150 °F, the samples were taken out of the furnace. Annealed copper billet samples 16 mm long were cut from a rod of diameter 25.4 mm. Before the experiment, a liquid lubricant was applied to the surfaces of the upper and lower dies. In order to observe underfill and flash formation, the first set of experiments was carried out using final dies without the preform die set. Figure 30 shows underfill and flash formation as predicted using FE simulation.

Figure 31 shows that using preform and final die sets, the part is fully formed. The maximum preform load and the maximum load for the final die obtained in the experiments were 800 kN and 1200 kN, respectively (Fig. 32). These values are in agreement with the forming loads obtained in the FEA simulations shown in Fig. 9, indicating that this methodology is suitable for designing preform dies. Validation of the developed

preform method was not carried out for steel samples because the maximum tonnage for the hydraulic press used was 150 tons, whereas the FE simulations of the rib-web part using AISI 1015 material indicated that a maximum forging load of 170 tons is needed for final-stage forging.

6 CONCLUSIONS

A new method for preform design based on shape resemblance has been presented. The proposed method is based on constructing a part slightly larger than the desired part and then performing a finite element simulation of the larger part with a reasonably guessed preform. Because the part has been enlarged and most forming defects (i.e. fold, underfill, flash) usually occur at or close to the boundary, defects will be confined to the enlarged portion. By backwards tracing of material flow on the desired part boundaries, a preform shape can be obtained. To verify the methodology, four case studies featuring 2D close die forging, 2D extrusion, and 2D upsetting were carried out. Experimental verification was also carried out for the Axisymmetric Rib-web part, which showed results similar to those obtained via the finite element method.

This study leads to the following conclusions:

(a) the developed preform design methodology has demonstrated that two or three FE iterations are sufficient to converge to a good preform shape for defect-free forming of a given part;
(b) the case studies presented have shown that this methodology can handle a variety of axisymmetric forging, extrusion, and upsetting/heading problems.

All the applications presented in this paper are 2D, but this preform design methodology could be extended to 3D parts. However, 3D parts will require more effort for mapping the track points in the preform design than would 2D parts. Further study is also needed to investigate the influence of the initial preform guess and variations in the construction of the larger part on the effective strain distribution and forming load.

REFERENCES

1 **Vemuri, K. R., Oh, S. I.,** and **Altan, T.** A knowledge-base system to automate blocker design. *Int. J. Mach. Tools Mf*, 1988, **29**(4), 505–518.
2 **Bariani, P.** and **Knight, W. A.** Computer-aided cold forging process design: a knowledge-based system approach to forming sequence generation. *Annls CIRP*, 1988, **37**, 243.
3 **Osakada, K., Yang, G. B., Nakamura, T.,** and **Mori, K.** Expert system for coldforging process based on FEM simulation. *Annls CIRP*, 1990, **39**, 249–252.
4 **Kim, H.** and **Altan, T.** Computer-aided part and processing-sequence design in cold forging. *J. Mater. Process. Technol.*, 1992, **33**, 57–74.
5 **Kim, H. S.** and **Im, Y. T.** Expert system for multi-stage cold forging process design with a redesigning algorithm. *J. Mater. Process. Technol.*, 1995, **54**, 271–285.
6 **Tisza, M.** Expert systems for metal forming. *J. Mater. Process. Technol.*, 1995, **53**, 423–432.
7 **Kim, H. S.** and **Im, Y. T.** Multi-stage cold forging process design with a searching algorithm. *Trans. NAMRC*, 1996, **24**, 161.
8 **Kim, H.** and **Altan, T.** Cold forging of steel-practical examples of computerized part and process design. *J. Mater. Process. Technol.*, 1996, **59**, 122.
9 **Osakada, K., Kado, T.,** and **Yang, G. B.** Application of AI-technique to planning of cold forging. *Annls CIP*, 1998, **37**(1), 239–242.
10 **Caporalli, A., Gileno, L. A.,** and **Button, S. T.** Expert system for hot forging design. *J. Mater. Process. Technol.*, 1998, **80–81**, 131–135.
11 **Kim, H. S.** and **Im, Y. T.** An expert system for cold forging process design based on a depth-first search. *J. Mater. Process. Technol.*, 1999, **95**, 262–274.
12 **Song, J. H.** and **Im, Y. T.** Development of a computer-aided-design system of cold forward extrusion of a spur gear. *J. Mater. Process. Technol.*, 2004, **153**, 821.
13 **Song, J. H.** and **Im, Y. T.** The applicability of process design system for forward extrusion of spur gears. *J. Mater. Process. Technol.*, 2007, **184**, 411–419.
14 **Bakhshi-Jooybari, M., Pillinger, I., Dean, T. A.,** and **Hartley, P.** Development of product and process comparison criteria for an intelligent knowledge-based system for forging die design. *Proc. IMechE, Part B: J. Engineering Manufacture*, 1996, **210**(B7), 565–578.
15 **Park, J. J., Rebelo, N.,** and **Kobayashi, S.** A new approach to preform design in metal forming with the finite element method. *Int. J. Mach. Tool Des. Res.*, 1983, **23**, 71–79.
16 **Kobayashi, S., Oh, S. I.,** and **Altan, T.** *Metal forming and finite element method*, 1989 (Oxford University Press, New York).
17 **Kim, N.** and **Kobayashi, S.** Preform design in H-shape cross section axisymmetric forging by finite element method. *Int. J. Mach. Tools Mf.*, 1990, **30**, 243–268.
18 **Zhao, G., Wright, E.,** and **Grandhi, R. V.** Forging preform design with shape complexity control in simulating backward deformation. *Int. J. Mach. Tools Mf.*, 1995, **35**, 1225–1239.
19 **Zhao, G., Wright, E.,** and **Grandhi, R. V.** Computer aided preform design in forging using the inverse die contact tracking method. *Int. J. Mach. Tools Mf.*, 1996, **36**, 755–769.
20 **Chang, C. C.** and **Bramley, A. N.** Forging preform design using a reverse simulation approach with the upper bound finite element procedure. *Proc. IMechE, Part C: J. Mechanical Engineering Science*, 2000, **214** (C1), 127–136. DOI: 10.1243/0954406001522868.

21 **Badrinarayanan, S.** and **Zabaras, N.** A sensitivity analysis for the optimal design of metal forming processes. *Computer Methods in Appl. Mechanics Engng*, 1996, **129**, 319–348.

22 **Fourment, L.** and **Chenot, J. L.** Optimal design for non-steady-state metal forming process-I: Shape optimization method. *Int. J. Numer. Methods Engng*, 1996, **39**, 33–50.

23 **Zhao, G., Wright, E.,** and **Grandhi, R. V.** Preform die shape design in metal forming using an optimization method. *Int. J. Numer. Methods Engng*, 1997, **40**, 1213–1230.

24 **Srikanth, A.** and **Zabaras, N.** Shape optimization and preform design in metal forming process. *Computer Methods in Appl. Mech. Engng*, 2000, **190**, 1859–1901.

25 **Zabaras, N., Ganapathysubramanian, S.,** and **Li, Q.** A continuum sensitivity method for the design of multi-stage metal forming processes. *Int. J. Mech. Sci.*, 2003, **45**, 325–358.

26 **Vieilledent, D.** and **Fourment, L.** Shape optimization of axisymmetric preform tools in forging using a direct differentiation method. *Int. J. Numer. Meth. Engng*, 2001, **52**, 1301–1321.

27 **Castro, C. F., Sousa, L. C., Antonio, C. A. C.,** and **Cesar de Sa, J. M. A.** An efficient algorithm to estimate optimal preform die shape parameters in forging. *Engng Comput.*, 2001, **18**, 1057–1077.

28 **Castro, C. F., Antonio, C. A. C.,** and **Sousa, L. C.** Optimization of shape and process parameters in metal forging using genetic algorithms. *J. Mater. Process Technol.*, 2004, **146**, 356–364.

29 **Thiyagarajan, T.** and **Grandhi, R. V.** 3D preform shape optimization in forging using reduced basis techniques. *Engng Optimization*, 2005, **37**, 797–811.

30 **Hong, J. T., Lee, S. R., Park, C. H.,** and **Yang, D. Y.** Iterative preform design technique by tracing the material flow along the deformation path application to piston forging. *Engng Computing*, 2006, **23**, 16–31.

31 **Nagpal, V.** Process design and finite element analysis software for metal forming. *Fastener Tech. Int. J.*, October 2009, 30—31.

32 **Bramfitt, B. L.** and **Hingwe, A. K.** Annealing of steel. *ASM Handbook*, 1991, Vol 4, p. 46 (ASM International, Materials Park, Ohio).

33 **Karadeniz, E.** Influence of different initial microstructure on the process of spheroidization in cold forging. *Mater. Des.*, 2008, **29**, 251–256.